Inorganic Chemistry Communications 110 (2019) 107598

Contents lists available at ScienceDirect

Inorganic Chemistry Communications

journal homepage: www.elsevier.com/locate/inoche

A nickel pyridine-selenolate complex for the photocatalytic evolution of hydrogen from aqueous solutions

An Xie[a], Yun-Wen Tao[c,*], Cheng Peng[b], Geng-Geng Luo[b,*]

[a] School of Materials Science and Engineering, Xiamen University of Technology, Xiamen 361021, China
[b] College of Materials Science & Engineering, Huaqiao University, Xiamen, Fujian 361021, China
[c] Department of Chemistry, Southern Methodist University, 3215 Daniel Avenue, Texas 75275-0314, USA

GRAPHICAL ABSTRACT

A nickel pyridine-selenolate complex is shown to be an active molecular photocatalyst for water splitting into hydrogen.

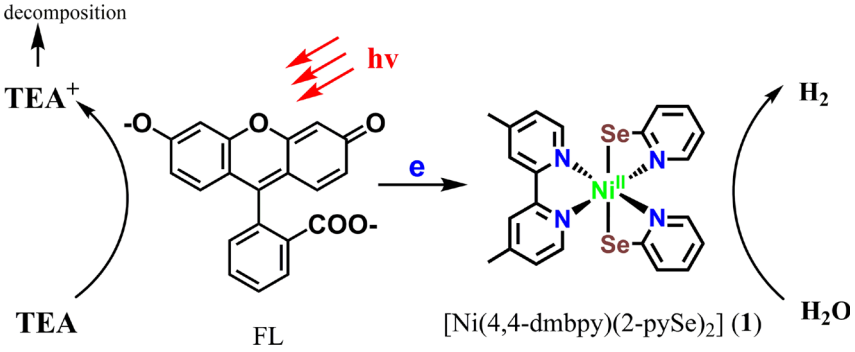

ARTICLE INFO

Keywords:
Nickel-selenolate complexes
Photocatalysis
Molecular catalysis
Crystal structure
Hydrogen evolution

ABSTRACT

A nickel pyridine-selenolate complex, [Ni(4,4′-dmbpy)(2-pySe)$_2$] (**1**, where 4,4′-dmbpy = 4,4′-dimethyl-2,2′-bipyridine, and 2-pySe = pyridine-2-selenolate), has been synthesized, and investigated for photocatalytic production of H_2 from aqueous solution. Electrochemical studies show that the nickel complex **1** can efficiently electrocatalyze H_2 evolution from weakly acidic solutions. Under visible-light irradiation ($\lambda > 420$ nm), the complex **1** displays impressive H_2 evolution activity with a TON of 1340 (based on a catalyst) in a noble-metal-free system, which contains fluorescein (Fl) as photosensitizer and triethylamine (TEA) as sacrificial electron donor in acetonitrile-water solution. It should be noted that complex **1** is the rare example of nickel pyridine-selenolate complex as molecular photocatalyst for water reduction.

Molecular hydrogen (H_2) is an ideal energy carrier for the future and solar water splitting into H_2 in natural photosynthesis represents a promising process to replicate in an artificial manner for clean and renewable fuel production. In this arena, [NiFe]-hydrogenases (H_2ase), a class of natural enzymes, are promising candidates because these H_2ases have inexpensive Ni and/or Fe atoms at the active sites, which can catalyze the reversible reduction of H^+ into H_2 with high efficiency comparable to the noble-metal Pt. However, these biological H_2ases have the large size and relative instability in nonbiological systems, underscoring the need for the design and synthesis of small-molecule

* Corresponding authors.
E-mail addresses: ywtao.smu@gmail.com (Y.-W. Tao), ggluo@hqu.edu.cn (G.-G. Luo).

https://doi.org/10.1016/j.inoche.2019.107598
Received 3 September 2019; Received in revised form 26 September 2019; Accepted 27 September 2019
Available online 21 October 2019

catalysts. Thus, in the past decades, intense work and significant effort has been made to develop nickel-based functional complexes ligated by N and/or S donor capable of reducing protons [1–3].

On the other hand, as a subclass of the [NiFe]-H_2ases, [NiFeSe]-H_2ases, structurally contain a terminal selenocysteine residue coordinated to the Ni center instead of a cysteine in the enzyme functional core. It is thought that such simple replacement of S with Se has already made [NiFeSe]-H_2ases have a high H_2 generation rate and tolerance to O_2 compared with other H_2ases [4]. This result has inspired many scientists to design and synthesize new Se-containing Ni complexes as catalysts for H_2 generation [5,6]. However, to date, there were rare examples applying nickel selenolate complexes as molecular photocatalyst for visible-light-driven H_2 generation.

As part of our ongoing research in Ni-based molecular catalysts for H_2 production [6,7], herein we report the synthesis and characterization of a new nickel(II) pyridine-selenolate complex, [Ni(4,4′-dmbpy)(2-pySe)$_2$] (**1**, where 4,4′-dmbpy = 4,4′-dimethyl-2,2′-bipyridine and 2-pySe = pyridine-2-selenolate), and investigate its photocatalytic H_2-evolution performance in aqueous solution.

Complex **1** was conveniently synthesized in two steps. First, 4,4′-dmbpy ligand was mixed with a nickel precursor ([Ni$(NO_3)_2$·6H_2O]). In a second step, 1,2-di(pyridin-2-yl)diselane was introduced into the precursor complex system in the presence of sodium borohydride. After purification by recrystallization, **1** was isolated as a dark-orange and air stable solid in 79% yield. The molecular structure of **1** is unambiguously established by single-crystal X-ray diffraction. As displayed in Fig. 1, the X-ray structure analysis revealed that the Ni(II) atom is coordinated by three bidentate ligands, i.e., by one N,N′-donor 4,4′-dmbpy ligand, and two N,Se-donor pyridine-2-selenolate (pySe) ligands, thus forming the distorted octahedral arrangement in the vicinity of the nickel center. The bond lengths of Ni—N and Ni—Se are in the range of 2.045(7)–2.076(8) Å and 2.611(2)–2.632(2) Å, respectively. The Ni-N distances are comparable to other octahedral Ni(II) complexes [8], while the average Ni-Se length (2.62 Å) is slightly longer than that in Ni-Se-Cys complex in D. baculatum [NiFeSe]-H_2ase (2.44 Å) [4a]. In **1**, the four-membered N,Se-chelate rings have a N—Ni—Se bond angle of ~ 69°, while for the five-membered N,N′-chelate ring involving bipyridine ligand the bite angle is about 78°. Thus, the smaller bite-angle of pyridine-selenolate ligand (∠N—Ni—Se vs. ∠N—Ni—N) indicates the existence of larger tension, which will be preferentially dechelated upon protonation during the catalytic process [9]. It is worth mentioning that **1** represents the first crystal structure of Ni^{II} complex ligated by pyridine-selenolate and bipyridine ligand. UV—Vis absorption spectrum of **1** in CH_3CN shows high-energy bands in the UV region with molar extinction coefficients ε on the order of 10^4 M^{-1} cm^{-1} (Fig. S1, in the Supporting Information), ascribed to spin-allowed intraligand $\pi \rightarrow \pi^*$ transitions [10].

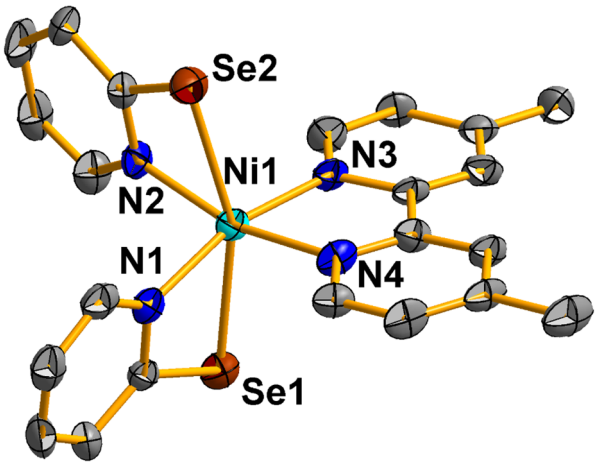

Fig. 1. ORTEP view of the synthesized Ni^{II} complex **1** with thermal ellipsoids drawn at the 50% probability level. All H atoms are omitted for clarity.

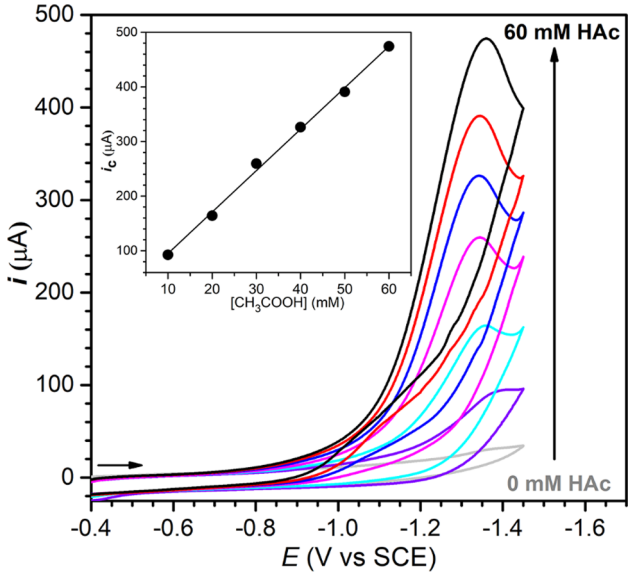

Fig. 2. CVs of 0.5 mM of **1** in CH_3CN/H_2O (1:1, v/v) without the presence of CH_3CO_2H (grey) and in the presence of increasing CH_3CO_2H concentrations (other colors) on a glassy carbon electrode. Inset: plot of i_{cat} taken from the peak plateau versus [CH_3CO_2H].

To examine **1** as potential electrocatalyst for H_2 production from aqueous solution, the weak acetic acid (CH_3CO_2H, pKa^{CH3CN} = 22.3) was added to **1** solution of 1:1 CH_3CN/H_2O and a usual three-electrode set-up using a glassy carbon working electrode is used. As shown in Fig. 2, the cyclic voltammetry (CV) experiments show significant current enhancements with an onset potential at −0.90 V (all potentials are quoted relative to SCE) and a half-wave potential of −1.19 V are afforded with various amounts of CH_3CO_2H, indicative of catalysis. A control experiment without **1** but with the same amount of added CH_3CO_2H in the same solvent mixture shows a negligible current rising. Under non-saturating acid conditions, the linear relationship between catalytic current (i_{cat}) and [CH_3CO_2H] suggests a first-order dependence of the catalytic rate on acid concentration. The H_2-evolving activity of **1** reaches an acid-independent region with more than 120 equiv of CH_3CO_2H, as indicated in the inset of Fig. 2.

Given that complex **1** can efficiently perform electrocatalytic production of H_2 from aqueous solution, we are especially concerned whether the complex is capable of photocatalytic reaction activities for H_2 generation. Photocatalytic experiments for H_2 production were conducted by adopting a classical three-component noble-metal-free system [11] in the presence of a triethamine (TEA) as the sacrificial donor, fluorescein (Fl) as the prototypical photosensitizer, and **1** as the molecular H_2-generating catalyst in a media of a CH_3CN/H_2O mixture (v/v = 1:1). Photolysis of a solution with visible light (λ > 420 nm) at 20 °C results in H_2 gas generation. The headspace gas is quantitatively analyzed by GC with a TCD detector. In the light-induced catalytic experiments, the pH value has a strong effect on the H_2-evolving activity [12]. Therefore, a series of 8 h photolysis experiments based on the systems containing **1** by changing the pH of the solution were performed to explore the effect of the pH media while keeping the component concentrations of 2×10^{-3} M Fl chromophore, 4×10^{-6} M catalyst **1**, and 0.36 M TEA in 1:1 CH_3CN/H_2O (Fig. 3). The pH value of each run was adjusted to the desired value by the addition of hydrochloric acid prior to addition of the Fl and **1**. The reaction has been found to be sensitive to the pH. The great decrease in amounts of H_2 at lower pH of 9.5 can be rationalized by the protonation of TEA to a considerable extent, which resulted in poor electron-donating ability [11]. At a higher pH of 12.3, the decrease concentrations of protons will

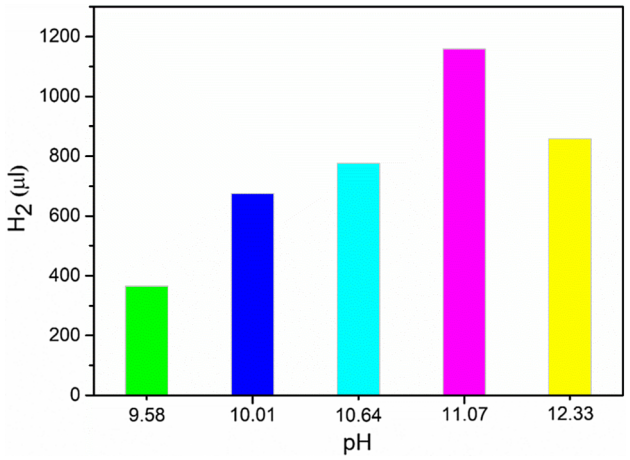

Fig. 3. Influence of pH on the photocatalytic of H_2 from a typical three-component system composed of **1** + Fl + TEA in 1:1 CH_3CN/H_2O after 8 h of irradiation using visible light irradiation (λ > 420 nm).

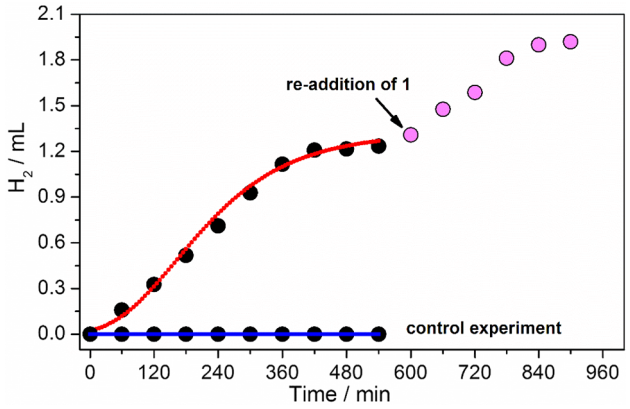

Fig. 4. H_2 production as a function of time and the regeneration of photocatalytic activity upon addition of catalyst **1**. Conditions: **1** (4×10^{-6} M), Fl (2×10^{-3} M) and TEA (0.36 M) in CH_3CN/H_2O (1:1, v/v, pH = 11.07), visible light irradiation (λ > 420 nm).

lead to a deceleration of efficiency of photogenerated H_2 [11,12]. In addition, the formation of the nickel hydride species is not favored at a higher pH.

As shown in Figs. 3 and 4, **1** is most active at pH 11.07 for photocatalytic H_2 production, which released a total amount of 1.2 mL H_2 (TON = 1340 with respect to a catalyst) after 8 h of irradiation. Control experiments revealed that negligible H_2 generation could be detected by GC outside of experimental error in the absence of any single molecular constituent (**1**, FL or TEA) in the system (Fig. 4), demonstrating that all the components make an essential contribution in the reaction for the evolution of H_2. Moreover, the reaction did not proceed when the catalytic reaction was performed under the same reaction conditions but in the absence of visible light, suggesting that light irradiation is a necessary component to provide the electrochemical driving force for electron transfer to achieve a fuel-producing catalysis. These experimental results suggest that **1** can promote the photocatalytic H_2 production. After 8 h of irradiation, the rate of H_2 evolution decreased obviously, indicate that at least one of component decompose. The addition of a fresh FL or TEA showed a negligible restoration of activity. However, after the readdition of an extra equiv. of catalyst **1**, the initial activity has restored. The results indicate the deactivation of the system is mainly limited by the decomposition of **1** under illumination (Fig. 4). It should be noted that there were rare cases employing nickel complexes ligated by selenolate ligands as molecular photocatalyst for visible-light-driven H_2 generation.

As we know, in three-component photocatalytic systems containing a H_2-evolving catalyst, a photosensitizer and an electron donor, the reduction of the catalyst to evolve hydrogen may occur by two intermolecular photochemically driven electron transfer steps [11–13]. One is that the H_2-evolving catalyst oxidatively quenches photoexcited Fl* to generate $[Fl]^{\bullet+}$. The other is that the electron donor TEA reductively quenches photoexcited FL* to produce $[Fl]^{\bullet-}$, which delivers an electron to the H_2-evolving catalyst for proton reduction to H_2. To determine the dominant reaction pathway in the system, the luminescence of the excited photosensitizer Fl*, in 1:1 CH_3CN/H_2O at pH 11.07 is undertaken as a function of both TEA and separately, **1** concentration (Fig. 5). Stern-Volmer analyses yielded the quenching constants for the system. The rate constants for reductive quenching of Fl* by TEA and oxidative quenching by **1** are 2.5×10^7 and 9.0×10^9 M^{-1} s^{-1}, respectively. As indicated by the reported Refs. [10,13], these results show that the quenching processes are diffusion controlled. Although the rate constant for oxidative quenching is ~ 400 times larger than that of reductive quenching, the reductive quenching process is still dominant given the much higher concentration of TEA (0.36 M) relative to **1** (4 μM).

For **1**, the CV test in the solution of 1:1 CH_3CN/H_2O shows no obvious reduction wave at potential less negative than −1.5 V (vs SCE), implying that **1** cannot accept an electron from $[Fl]^{\bullet-}$ (-1.3 V) [13]. Thus, based on the previous Ref. [13], a protonated form of **1** may be the electron acceptor. The effect of protonation of **1** was examined by monitoring the electronic absorption spectral changes of **1** upon addition of acid. As illustrated in Fig. 6, in acidic solution, the original band at 350 nm of **1** gradually loses intensity and new absorption peaks are

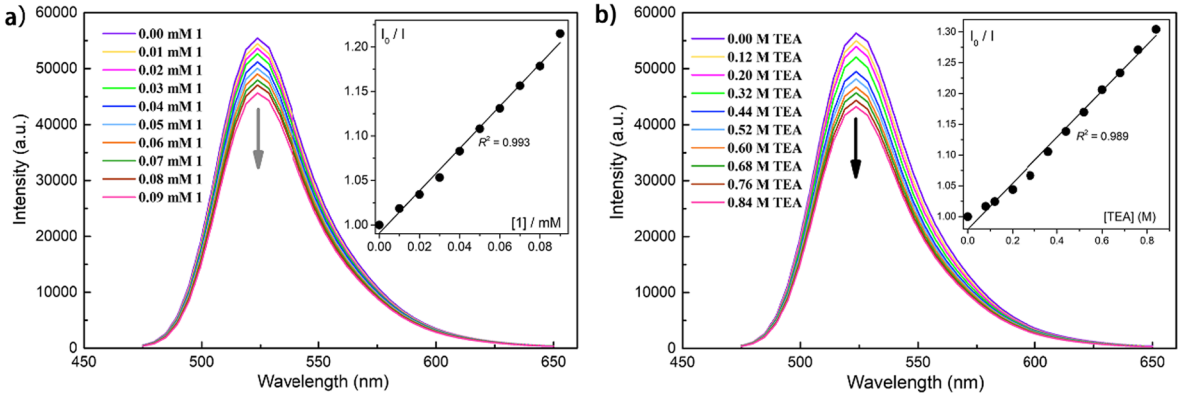

Fig. 5. (a) Emission spectra of Fl (10^{-5} M) as a function of added catalyst **1** in 1:1 CH_3CN/H_2O at pH 11.07. Inset: Stern-Volmer plot of quenching by catalyst **1** (the best-fit equation of the Stern-Volmer plot is $y = (9.0 \times 10^9)x + 1$). (b) Emission spectra of Fl (10^{-5} M) as a function of added TEA in 1:1 CH_3CN/H_2O at pH 11.07. Inset: Stern-Volmer plot of quenching by TEA (the best-fit equation of the Stern-Volmer plot is $y = (2.45 \times 10^7)x + 1$).

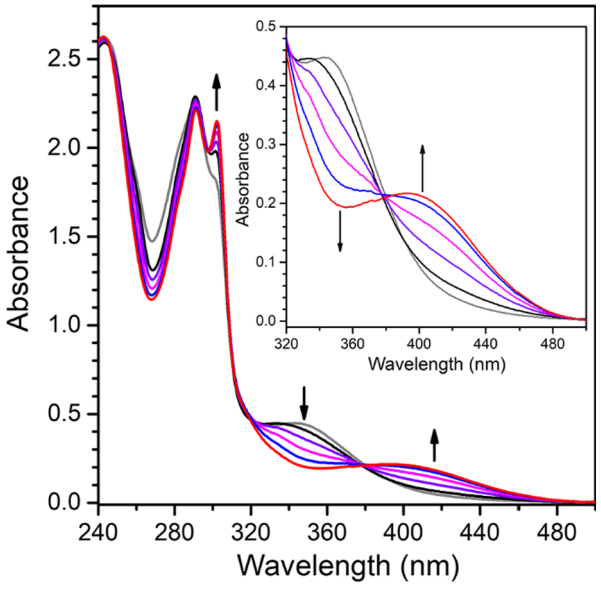

Fig. 6. UV–vis absorption spectral changes after the sequential addition of proton source (0, 0.6, 0.8, 1.0, 1.2, 1.4 equiv.) to a solution of **1** in CH_3CN.

observable at ~ 303 and 408 nm with conserved isosbestic points at ~ 320 and 380 nm, indicating **1** converts to its protonated species [10]. In addition, as implied by the previous reference [13], the UV/vis spectrum of **1** also undergoes an obvious pH-dependent change in CH_3CN/H_2O (1:1) (Fig. S2, in the Supporting Information). Considering the electrochemical and photochemical studies, a possible catalytic pathway is briefly documented based on well-established studies [10,13]. Photocatalytic H_2 production reaction starts with the quenching the excited-state of Fl (Fl*). In the presence of an electron donor TEA, the Fl* is reductively quenched, providing a reduced sensitizer, that is anionic form $Fl^{\bullet-}$. The $Fl^{\bullet-}$ delivers an electron to the protonated catalyst unit, where H_2 can be produced. However, more studies are further needed to reveal the mechanism of the nickel catalyst for photocatalytic H_2 production.

In summary, a new nickel pyridine-selenolate complex, [Ni(4,4′-dmbpy)(2-pySe)$_2$] (**1**), has been synthesized and characterized by single-crystal X-ray diffraction. The nickel-selenolate complex was found to be active for electrocatalytic H_2 production when employing acetic acid as a very inexpensive proton source. In the presence of organic photosensitizer Fl and an electron donor TEA, the complex **1** could evolve H_2 from CH_3CN/H_2O (1:1, v/v) with a TON of 1340 when exposed to visible light irradiation. This study represents a new paradigm for the construction of noble-metal-free catalyst by using nickel (II)-selenolate complexes for solar driven H_2 generation.

Declaration of Competing Interest

The authors declared that there is no conflict of interest.

Acknowledgments

We are grateful to the National Natural Science Foundation of China (21641011), the Natural Science Foundation of Fujian Province (2015 J01053 and 2017 J01016), the Fujian Key Laboratory of Functional Materials and Applications (Xiamen University of Technology, fma2017107).

Appendix A. Supplementary material

Supplementary data to this article can be found online at https://doi.org/10.1016/j.inoche.2019.107598.

References

[1] (a) S. Fukuzumi, Y.-M. Lee, W. Nam, Thermal and photocatalytic production of hydrogen with earth-abundant metal complexes, Coord. Chem. Rev. 355 (2018) 54–73;
(b) W.T. Eckenhoff, Molecular catalysts of Co, Ni, Fe, and Mo for hydrogen generation in artificial photosynthetic systems, Coord. Chem. Rev. 373 (2018) 295–316;
(c) T. Xu, D.-F. Chen, X.-L. Hu, Hydrogen-activating models of hydrogenases, Coord. Chem. Rev. 303 (2015) 32–41;
(d) G.-G. Luo, H.-L. Zhang, Y.-W. Tao, Q.-Y. Wu, D. Tian, Q.-C. Zhang, Recent progress in ligand-centered homogeneous electrocatalysts for hydrogen evolution reaction, Inorg. Chem. Front. 6 (2019) 343–354.

[2] (a) H. Rao, W.-Q. Yu, H.-Q. Zheng, J.-L. Bonin, Y.-T. Fan, H.-W. Hou, Highly efficient photocatalytic hydrogen from nickel quinolinethiolate complexes under visible light irradiation, J. Power Sources 324 (2016) 253–260;
(b) B.-B. Zhang, L.-C. Sun, artificial photosynthesis: opportunities and challenges of molecular catalysts, Chem. Soc. Rev. 48 (2019) 2216–2264;
(c) J.-W. Wang, W.-J. Liu, D.-C. Zhong, T.-B. Lu, Nickel complexes as molecular catalysts for water splitting and CO_2 reduction, Chem. Soc. Rev. 378 (2019) 237–261.

[3] (a) A.J. Esswein, D.G. Nocera, Hydrogen production by molecular photocatalysis, Chem. Rev. 107 (2007) 4022–4047;
(b) A. Xie, J. Zhu, G.-G. Luo, Efficient electrocatalytic and photocatalytic hydrogen evolution using a linear trimeric thiolato complex of nickel, Int. J. Hydrogen Energ. 43 (2018) 2772–2780.

[4] (a) A. Parkin, G. Goldet, C. Cavazza, J.C. Fontecilla-Camps, F.A. Armstrong, The difference a Se makes? Oxygen-tolerant hydrogen production by the [NiFeSe]-hydrogenase form desulfomicrobium baculatum, J. Am. Chem. Soc. 130 (2008) 13410–13416;
(b) M.C. Marques, C. Tapia, O. Gutiérrez-Sanz, A.R. Ramos, K.L. Keller, J.D. Wall, A.L. De Lacey, P.M. Matias, I.A.C. Pereira, The direct role of selenocysteine in [NiFeSe] hydrogenase maturation and catalysis, Nat. Chem. Bio. 13 (2017) 544–550.

[5] (a) C. Wombwell, E. Reisner, Synthetic active site model of the [NiFeSe] hydrogenase, Chem. Eur. J. 21 (2015) 8096–8104;
(b) C. Wombwell, C.A. Caputo, E. Reisner, [NiFeSe]-hydrogenase chemistry, Acc. Chem. Res. 48 (2015) 2858–2865 and references therein.

[6] Z.-H. Pan, Y.-W. Tao, Q.-F. He, Q.-Y. Wu, L.-P. Cheng, Z.-H. Wei, J.-H. Wu, J.-Q. Lin, D. Sun, Q.-C. Zhang, D. Tian, G.-G. Luo, The difference Se makes: a bio-inspired dppf-supported nickel selenolate complex boosts dihydrogen evolution with high oxygen tolerance, Chem. Eur. J. 24 (2018) 8275–8280.

[7] G.-G. Luo, Y.-H. Wang, J.-H. Wang, J.-H. Wu, R.-B. Wu, A square-planar nickel dithiolate complex as an efficient molecular catalyst for the electro- and photoreduction of protons, Chem. Commun. 53 (2017) 7007–7010.

[8] R. Castro, M.L. Durán, J.A. García-Vázquez, J. Romero, A. Sousa, A. Castiñeiras, W. Hiller, J. Strähle, Direct electrochemical synthesis of pyridine-2-thionato complexes of nickel(II): the crystal structure of (2,2′-bipyridine)bis(pyridine-2-thionato) nickel(II)-2,2′-bipyridine(2/1), J. Chem. Soc., Dalton Trans. 531–533 (1990).

[9] A.L. Petrou, A.D. Koutselos, H.S. Wahab, W. Clegg, R.W. Harrington, R.A. Henderson, Kinetic and theoretical studies on the protonation of [Ni(2-SC_6H_4N){$PhP(CH_2CH_2PPh_2)_2$}]$^+$: nitrogen versus sulfur as the protonation site, Inorg. Chem. 50 (2011) 847–857.

[10] Z.-J. Han, L.-X. Shen, W.W. Brennessel, P.L. Holland, R. Eisenberg, Nickel pyridinethiolate complexes as catalysts for the light-driven production of hydrogen from aqueous solutions in noble-metal-free systems, J. Am. Chem. Soc. 135 (2013) 14659–14669.

[11] (a) G.-G. Luo, Z.-H. Pan, J.-Q. Lin, D. Sun, Tethered sensitizer-catalyst noble-metal-free molecular devices for solar-driven hydrogen generation, Dalton Trans. 47 (2018) 15633–15645;
(b) W.T. Eckenhoff, R. Eisenberg, Molecular systems for light driven hydrogen production, Dalton Trans. 41 (2012) 13004–13021;
(c) X.-C. Li, G.-G. Luo, K. Fang, J.-W. Zhou, Q.-H. Zhao, R.-B. Wu, Photocatalytic hydrogen generation based on noble-metal-free BODIPY or Aza-BODIPY organic dyes as photosensitizers, Scientia Sinica Chimica 45 (2015) 843–854;
(d) Y. Zhao, Y.H. Wang, Q.-Y. Wu, J.-Q. Lin, S.-H. Wu, W.-J. Hou, R.-B. Wu, G.-G. Luo, New tricks for an old dog: Visible light-driven hydrogen production from water catalyzed by fac- and mer-geometrical isomers of tris(thiosemicarbazide)cobalt(III), Chinese J. Catal. 3 (2018) 517–526.

[12] (a) G.-G. Luo, K. Fang, J.-H. Wu, J. Mo, Photocatalytic water reduction from a noble-metal-free molecular dyad based on a thienyl-exapnded BODIPY photosensitizer, Chem. Commun. 51 (2015) 12361–12364;
(b) G.-G. Luo, H. Lu, X.-L. Zhang, J.-C. Dai, J.-H. Wu, J.-J. Wu, The relationship between the boron dipyrromethene (BODIPY) structure and the effectiveness of homogeneous and heterogeneous solar hydrogen-generating systems as well as DSSCs, Phys. Chem. Chem. Phys. 17 (2015) 9716–9729;
(c) A. Xie, X.-L. Liu, Y.-C. Xiang, G.-G. Luo, a homogeneous molecular system for the photogeneration of hydrogen from water based on a [RuII(bpy)3]2+ photosensitizer and a phthalycyanine cobalt catalyst, J. Alloy. Compd. 717 (2017) 226–231;
(d) G.-G. Luo, K. Fang, J.-H. Wu, J.-C. Dai, Q.-H. Zhao, Noble-metal-free BODIPY-cobaloxime photocatalysts for visible-light-driven hydrogen production, Phys. Chem. Chem. Phys. 16 (2014) 23884–23894.

[13] Z.-J. Han, W.R. McNamara, M.-S. Eum, P.L. Holland, R. Eisenberg, A nickel thiolate catalyst for the long-lived photocatalytic production of hydrogen in a noble-metal-free system, Angew. Chem. Int. Ed. 51 (2012) 1667–1670.